



Insights into the structure of cutin and cutan from *Agave americana* leaf cuticle using HRMAS NMR spectroscopy

Ashish P. Deshmukh¹, André J. Simpson², Christopher M. Hadad,
Patrick G. Hatcher^{*}

Department of Chemistry, Newman and Wolfrom Laboratory, The Ohio State University, 100 West 18th Avenue, Columbus, OH 43210, United States

Received 16 August 2004; accepted 11 February 2005
(returned to author for revision 26 October 2004)
Available online 27 April 2005

Abstract

The structure of cutan, and a cutin/cutan mixture from the *Agave americana* leaf cuticle is herein described by use of the technique of one and two-dimensional high-resolution magic angle spinning (HRMAS) NMR spectroscopy, with added information from solid-state ¹³C cross-polarization magic angle spinning (CPMAS) and Bloch decay NMR spectroscopy. Cutin in the cutin/cutan mixture is found to contain ester functionalities, in line with previous degradative approaches. Furthermore, epoxy groups, free primary alcohols and carboxylic acid groups are also observed in cutin. A significant new finding is the evidence for α -branched fatty acids/esters in cutin. Cutan has mainly free primary hydroxyls, as well as long-chain carboxylic acids, which have been previously predicted to form ester linkages with tri-hydroxylated benzene units. Another significant finding in cutan is the evidence for benzenecarboxylic acids that are ester linked with fatty alcohols. The long-chain polymethylenic groups in cutan are shown to express a high degree of crystallinity similar to that observed in soil organic matter.

© 2005 Elsevier Ltd. All rights reserved.

1. Introduction

Microorganisms degrade labile fractions in plant residues to CO₂, and the resistant components are stabi-

lized in the form of macromolecular humic substances in soils and sediments by a process that is described as 'selective preservation' of resistant biomolecules (Derenne and Lageau, 2001). Studies on organic matter in soils and sediments (SOM) as well as fossil fuels have shown that they are rich in long-chain polymethylenic functional groups (Nip et al., 1986a,b; Tegelaar et al., 1991, 1995; Collinson et al., 1994; van Bergen et al., 1994). In terrestrial systems, these components are believed to derive from plant cuticles containing the biopolymers cutin and cutan, and suberized parts of plant organs containing suberin (Nierop, 1998). It has also been shown that the aliphatic carbon content increases with increasing SOM decomposition (Balduck et al.,

^{*} Corresponding author. Tel.: +1 614 688 8799; fax: +1 614 688 5920.

E-mail address: hatcher@chemistry.ohio-state.edu (P.G. Hatcher).

¹ Current address: Department of Geosciences, Princeton University, Princeton, NJ 08544, United States.

² Current address: Department of Physical and Environmental Sciences, The University of Toronto, Scarborough College, 1265 Military Trail, Toronto, Ont., Canada M1C 1A4.

1997), which shows that these components are diagenetically resistant and survive unaltered over time, although it has been suggested that cutin does not show a high level of persistence in some soils (Kögel-Knabner et al., 1989).

Most cuticular matrices are made up of extractable waxes, and non-extractable polymeric lipid components, cutin and cutan. Cutin, a polyester, is depolymerized and solubilized upon saponification, while cutan is the non-saponifiable and non-extractable polymer found in certain cuticles. While some cuticles have only cutin, and no cutan (e.g., *Lycopersicon esculentum*, i.e., tomato fruit); others have only cutan (e.g., *Beta vulgaris*); and some others may have both (e.g., *Agave americana* leaf) (Jeffree, 1996).

Studies involving depolymerization of cutins using reactions such as alkaline hydrolysis, transesterification, and hydrogenolysis with LiAlH_4 in THF, followed by identification by gas chromatography-mass spectrometry (GC-MS) after derivatization, indicate that cutins are composed of C_{16} and C_{18} hydroxy and epoxy fatty acids (Kolattukudy, 1980). Monomer concentration is found to be species-dependent (Holloway, 1984) and dependent on the age of the cuticle (Riederer and Schonherr, 1988). The literature on the structure of cutin has been reviewed extensively (Kolattukudy, 1980, 1984, 2001, 2002; Holloway, 1984, 1994; Blee, 2002).

A. americana is a xerophytic monocotyledon whose leaves have a thick cuticle that is known to contain both cutin and cutan. Depolymerization studies indicate that *A. americana* cutin contains mainly C_{18} fatty acid derived monomers such as 9,10,18-trihydroxyoctadecanoic acid; 9,10-epoxy-18-hydroxyoctadecanoic acid; and 10,16-dihydroxyhexadecanoic acid (Espelie et al., 1982). The resistant residue that remains after depolymerization (saponification) of cutin is cutan, whose structure is only partially understood. Pyrolysis gas chromatography-mass spectrometry (Py-GC-MS) of *A. americana* cutan yields a homologous series of *n*-alkanes, *n*-alk-1-enes, and α,ω -alkadienes (Nip et al., 1986a,b; Tegelaar et al., 1989), which are thought to derive from thermal degradation of the polymethylene chains. Tetramethylammonium hydroxide (TMAH) thermochemolysis of *A. americana* cutan gives monomeric products that include fatty acid methyl esters (FAMES) of varying chain lengths (C_{15} – C_{31} , with a high concentration of C_{27} – C_{31}), a number of 1,3,5-trimethoxylated benzene derivatives, and a few benzene carboxylic acid derivatives (McKinney et al., 1996). Using the TMAH data in combination with the ^{13}C cross-polarization magic angle spinning nuclear magnetic resonance spectroscopy (CPMAS NMR) data, a structure for the biopolymer with a backbone of 1,3,5-trihydroxylated aromatic rings was proposed. It is believed that the hydroxyl groups on the aromatic rings form ester linkages

with fatty acids (McKinney et al., 1996). However, there is not enough information to predict the nature of the cross-link between the aromatic rings.

Schouten et al. (1998) subjected *A. americana* cutan to ruthenium tetroxide (RuO_4) oxidation, and a number of monocarboxylic acids (C_{16} – C_{34})- and α,ω -dicarboxylic acids (mainly C_9 , but also C_{26} – C_{34}) were obtained. Based on reactions with model compounds, this technique was found to cleave alkyl chains of aromatic rings, double bonds, and ethers. The unknown cross-link between aromatic rings was proposed to be a C_7 -link, which upon RuO_4 treatment gives the C_9 dicarboxylic acid. Schouten et al. (1998) believe that the C_{26} – C_{34} dicarboxylic acids are esterified at both ends with aromatic hydroxyl groups, which revert to the C_{26} – C_{34} dicarboxylic acids upon treatment with RuO_4 .

Villena et al. (1999) used exhaustive ozonolysis for solubilizing *A. americana* cutan, followed by oxidative cleavage of the ozonides and GC-MS analysis of the resulting acids after derivatization. The major products are C_4 – C_9 α,ω -dicarboxylic acids (71%), which the authors believe, are derived from double bonds and ethers based on changes in the infrared spectra. In addition, X-ray diffraction studies show narrow basal distances, thus suggesting that cutan is highly cross-linked.

Degradative studies are invasive and are therefore able to provide only inferences about cross-linking and other kinds of connectivities between monomers. Insolubility of the cuticular biopolymers has made it difficult for solution-state NMR techniques to be applied for structure determination. High-resolution magic angle spinning (HRMAS) NMR spectroscopy allows for the analysis of materials that swell, become partially soluble, or form true solutions in a solvent even when some solids are still present (Keifer et al., 1996; Millis et al., 1997). Stark et al. (2000) and Fang et al. (2001) used heterocorrelated multiple-quantum coherence (HMQC) NMR spectroscopy for comparing the structure of intact lime cutin swelled in dimethylsulfoxide (DMSO) with that of an oligomer (obtained by selective hydrolysis of hindered esters using iodotrimethylsilane) dissolved in CHCl_3 . The quantitative nature of the technique was confirmed by comparing spectra from dry and wet cutin (Stark et al., 2000). In a recent study (Deshmukh et al., 2003) we utilized two-dimensional HRMAS spectroscopy to identify some new cross-links and structural units in tomato cutin. CPMAS NMR spectroscopy has been used to identify the major carbon functionalities present in intact biopolymers, but two-dimensional techniques are essential for resolution of overlapping signals.

We report here a one- and two-dimensional HRMAS NMR study coupled with a one-dimensional CPMAS and Bloch decay ^{13}C study for characterization of the molecular architecture of (a) a cutin/cutan mixture,

and (b) cutan, isolated from *A. americana* leaf cuticle. We examined the cutin/cutan mixture to learn about cutin, because cutin could not be isolated independently of cutan from the *Agave* cuticle. One-dimensional ^1H HRMAS, two-dimensional total correlation spectroscopy (TOCSY), heteronuclear single quantum coherence (HSQC), and nuclear overhauser effect spectroscopy (NOESY) are performed on the biopolymers swollen in DMSO. Detailed through-bond connectivities and assignments are possible based on the data obtained. To our knowledge this is the first published account of HRMAS NMR spectroscopic structural analysis of cutin and cutan from *A. americana* leaves.

2. Materials and methods

2.1. Isolation of cutan from *A. americana* leaves

A. americana leaves were cut into small pieces (approximately 4 cm \times 4 cm), split into half, and the fleshy interiors were removed before suspending them in a solution of oxalic acid (0.4% w/v) and ammonium oxalate (1.6% w/v) at 40 °C for 2–3 days. The cuticles were easily separated from the bulk of the leaf and resuspended in a fresh oxalic acid and ammonium oxalate solution for one day to remove any associated matter. Cuticles were washed, freeze-dried, and ground in liquid nitrogen. Dried and ground cuticles were solvent extracted successively with chloroform, methanol, and 1:1 chloroform/methanol at gentle reflux for 12 h. The extraction was repeated three times until the dried extracts were free of dissolved material. The solvent extracted residue was treated with 1% KOH in 96% methanol for 2 h for removal of polyester cutin (Hol-loway, 1984). The washed and dried residue remaining after saponification was treated with 4.5% sodium paraperiodate solution (pH adjusted to 4.1 with acetic acid) for 12 h, followed by refluxing in H_2O for 3 h to remove any residual polysaccharides (Zelibor et al., 1988). The residue was washed and freeze-dried to obtain cutan.

2.2. Isolation of cutin/cutan mixture from *A. americana* leaves

Solvent extracted *A. americana* cuticles obtained as before, were treated with 4.5% sodium paraperiodate solution (pH adjusted to 4.1 with acetic acid) for 12 h. The residue was separated by filtration, resuspended in H_2O , and refluxed for 2 h (Zelibor et al., 1988). This treatment removed the polysaccharides in the material, and the residue contained only the cutin and cutan biopolymers. Cutin could not be isolated in its pure form from cutan.

2.3. NMR spectroscopy

Solid-state CPMAS ^{13}C NMR spectra using the ramp-cross polarization (CP) technique (Hediger et al., 1993), and two-pulse phase modulated (TPPM) decoupling (Bennett et al., 1995) technique, were obtained with a Bruker 300 MHz NMR-spectrometer (Bruker Analytic GmbH, Germany). The following optimized experimental parameters were used: ramp-CP contact time of 2 ms; recycle delay time of 1 second; sweep width of 27 kHz (368 ppm) and line broadening of 50 Hz. 90°H and ^{13}C pulse lengths were under 5 μs . The chemical shifts were referenced to the carboxyl signal of glycine as an external secondary standard with a shift of 176.03 ppm. Freeze-dried samples were placed in a 4 mm rotor, and spun at a frequency of 13 kHz at the magic angle (54.7° to the magnetic field). A contact time of 2 ms was determined to be optimum for all types of carbon functionalities. The Bloch decay (BD) MAS ^{13}C NMR spectra were acquired using an 18° pulse angle and a recycle delay of 2 s.

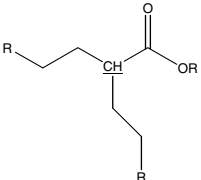
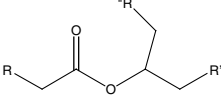
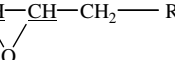
HRMAS NMR experiments were carried out on a Bruker Avance 600 MHz DRX spectrometer, fitted with a ^1H , ^{13}C , ^{15}N HRMAS probe. Sample (~ 30 mg) was swollen in $\text{DMSO-}d_6$ and packed into a 4 mm Zirconia rotor with a Kel-F cap. All spectra were obtained using 9 kHz spinning speed. Proton spectra were collected with composite pulse presaturation using 256 scans, 25 ppm sweep width, and 2 s recycle delays. For the *A. americana* cutan, a T_2 filter was created with a CPMG sequence, with presaturation, to create a delay of 60 μs , to help reduce baseline role. TOCSY {256 scans, TD (F_1) 1024, TD (F_2)} were acquired using time proportional phase incrementation (TPPI), and a mixing time of 50 ms. HSQC {196 scans, TD (F_1) 1024, TD (F_2) 512, $J^1(^1\text{H}-^{13}\text{C})$ 145 Hz} were acquired using sensitivity enhancement and gradients for coherence selection with decoupling during acquisition. All the two-dimensional datasets were processed using sine-squared functions with phase shifts of 90° in both dimensions. NOESY {512 scans, TD (F_1) 1024, TD (F_2)} were acquired using time proportional phase incrementation (TPPI), and a mixing time of 75 ms.

3. Results and discussion

3.1. *Agave* cutin/cutan mixture

CPMAS ^{13}C solid-state NMR spectroscopy is a technique that is useful for studying carbon functionalities in insoluble samples, but gives lines that are broader than those observed for materials in solution, mainly from the chemical shift anisotropy and the lack of molecular motion. In HRMAS techniques, one utilizes conventional liquids NMR pulse sequences to obtain signals

Table 1
Carbon and proton pairs identified in *Agave americana* cutan and cutin/cutan mixture with respective chemical shifts (ppm)

Symbol	Type	¹ H shift (ppm)	¹³ C shift (ppm)
A ₁	$\underline{\text{CH}_3}\text{-CH}_2\text{-CH}_2\text{-CH}_2\text{-R}$	0.8	14
A ₂	$\text{CH}_3\text{-CH}_2\text{-}\underline{\text{CH}_2}\text{-CH}_2\text{-R}$	1.3	30
B ₁	$\text{R-CH}_2\text{-CH}_2\text{-CH}_2\text{-CO-O-}\underline{\text{CH}_2}\text{-CH}_2\text{-CH}_2\text{-R}$	4.0	67
B ₂	$\text{R-CH}_2\text{-CH}_2\text{-CH}_2\text{-CO-O-CH}_2\text{-}\underline{\text{CH}_2}\text{-CH}_2\text{-R}$	1.5	30
B ₃	$\text{R-CH}_2\text{-CH}_2\text{-CH}_2\text{-CO-O-CH}_2\text{-CH}_2\text{-}\underline{\text{CH}_2}\text{-R}$	1.2	26
C ₁	$\text{R-CH}_2\text{-CH}_2\text{-}\underline{\text{CH}_2}\text{-CO-O-CH}_2\text{-CH}_2\text{-CH}_2\text{-R}$	2.3	34
C ₂	$\text{R-CH}_2\text{-}\underline{\text{CH}_2}\text{-CH}_2\text{-CO-O-CH}_2\text{-CH}_2\text{-CH}_2\text{-R}$	1.7	22
D ₁	$\text{R-CH}_2\text{-CH}_2\text{-}\underline{\text{CH}_2}\text{-OH}$	3.3	63
D ₂	$\text{R-CH}_2\text{-}\underline{\text{CH}_2}\text{-CH}_2\text{-OH}$	1.4	34
D ₃	$\text{R-}\underline{\text{CH}_2}\text{-CH}_2\text{-CH}_2\text{-OH}$	1.3	26
F ₁	$\text{R-CH}_2\text{-}\underline{\text{CH}_2}\text{-CO}_2\text{H}$	2.2	36
F ₂	$\text{R-}\underline{\text{CH}_2}\text{-CH}_2\text{-CO}_2\text{H}$	1.6	25
G		2.4	45
H		4.8	74
J	$\text{Ar-CO-O-}\underline{\text{CH}_2}\text{-CH}_2\text{-R}$	4.2	67
K	$\text{R-CH}_2\text{-}\underline{\text{CH}}\text{-CH-CH}_2\text{-R}$ 	2.7	56
L	$\text{R-CH}_2\text{-}\underline{\text{CH}}\text{=CH-CH}_2\text{-R}$	5.25	130

from solid materials whose molecular mobilities have been modified to narrow the lines broadened mainly by dipole–dipole interactions in solids. Materials swollen in DMSO have enhanced molecular mobility, and magic angle spinning removes or minimizes effects of chemical shift anisotropy, dipole–dipole interactions and magnetic susceptibility line broadening (Keifer et al., 1996; Millis et al., 1997; Stark et al., 2000; Fang et al., 2001).

Using two-dimensional techniques, we identify carbons and protons that fall into groups on the basis of their structures as A-type (terminal methyls

and main-chain methylenes), B-type (methylenes attached to the oxygen (O)-side of an ester), C-type (methylenes attached to the carbonyl (C=O) side of an ester), D-type (methylenes in free primary alcohols), F-type (methylenes in free fatty acids), G-type (methines in α -branched carboxylic acids/esters), H-type (methines attached to ester-linked mid-chain hydroxyls), J-type (methylenes attached to the oxygen (O)-side of esters between aliphatic alcohols and aromatic carboxylic acids), K-type (methines in epoxide groups), and L-type (methines in olefinic linkages) (Table 1).

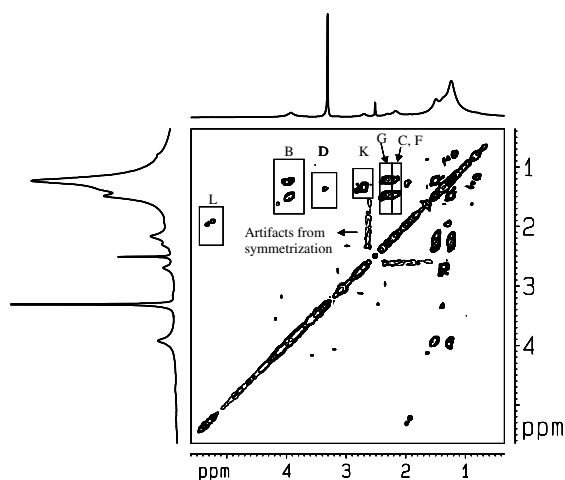


Fig. 1. High resolution magic angle spinning (HRMAS) ^1H - ^1H total correlation spectroscopy (TOCSY) NMR spectrum of *Agave americana* cutin/cutan mixture, swollen in $\text{DMSO-}d_6$, while spinning at 9 kHz.

TOCSY identifies through bond couplings between protons in the same spin system. Figure 1 shows the HRMAS TOCSY spectrum for the *Agave* cutin/cutan mixture. In this sample, which is dominated by signals from the polyester cutin, esters are identified easily. For B-type resonances (Table 1), the cross-peak at 4.0 ppm is from protons on methylenes (CH_2) directly attached to the oxygen atom of esters (B_1), which is further coupled to protons with chemical shift 1.5 ppm (CH_2s β to the O, B_2), and 1.2 ppm (CH_2s γ to the O, B_3). The cross-peak at 2.2 to 2.3 ppm is from protons on CH_2s that are directly attached to carbonyls ($\text{C}=\text{O}$) in ester or carboxylic acid functional groups (C or F-type). These CH_2s are coupled to protons at 1.5 ppm (CH_2s

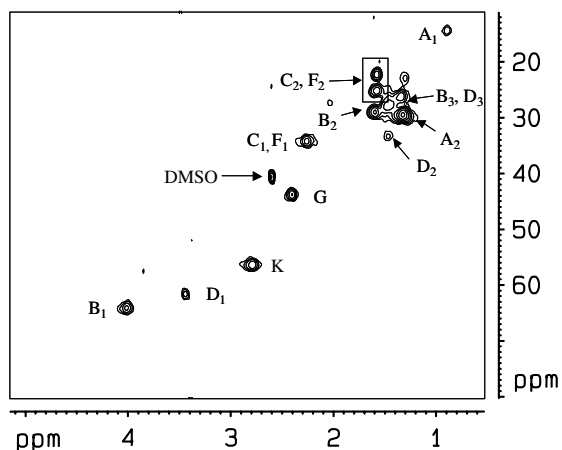


Fig. 2. High resolution magic angle spinning (HRMAS) ^1H - ^{13}C heteronuclear single quantum coherence (HSQC) NMR spectrum of *Agave americana* cutin/cutan mixture, swollen in $\text{DMSO-}d_6$, while spinning at 9 kHz.

β to CO) and 1.2 ppm (CH_2s γ to CO). This, in addition to the HSQC cross-peaks discussed below (Fig. 2), is direct evidence for the expected presence of ester type functionalities in cutin of the *Agave* cutin/cutan mixture. Primary alcohols are present as indicated by the peak at 3.3 ppm (D-type) from protons in CH_2 units directly bonded to free terminal hydroxyls (D_1), which couple to protons at 1.4 ppm (CH_2s β to OH, D_2). This correlates well with known *Agave* cutin monomers, such as 9,10,18-trihydroxyoctadecanoic acid, 9,10-epoxy-18-hydroxyoctadecanoic acid, and 10,16-dihydroxyhexadecanoic acid (Espelie et al., 1982), that have primary alcohol groups. The cross-peak at 2.7 ppm is from methine protons (CH) that are directly involved in epoxide formation (K-type), which are coupled to protons at 1.3 ppm (α - to epoxide, see also cross-peak K in Fig. 2). This correlates well with products containing epoxides obtained from depolymerization. Epoxides are found only in cutin, since these signals are absent in the spectra obtained for cutan (see later). The cross-peak at 5.2 ppm is from protons on olefinic carbons (L-type), which couple with protons at 2.0 ppm (α to double bond).

The TOCSY spectrum of *Agave* cutin/cutan mixture (Fig. 1) also exhibits a cross-peak at 2.4 ppm (G) in addition to the one at 2.2 ppm from straight chain fatty acids/esters (C/F). This peak at 2.4 ppm is from methines that are attached to carboxyl groups in α -branched fatty acids/esters (structure G, depicted in Table 1). Such methines have an alkyl substituent in addition to the carboxyl group. These methine protons couple with peaks at 1.5 ppm (β CH_2) and 1.2 ppm (γ CH_2). There is further confirmation for this peak from the cross-peak seen in the HSQC spectrum of the *Agave* cutin/cutan mixture, which shows the chemical shift of attached carbons as being 45 ppm (shown later). Such a peak at 2.4 ppm has also been observed in the HRMAS spectra of tomato cutin (Deshmukh et al., 2003). Fang et al. (2001) observed a similar peak in the ^1H NMR spectra of lime cutin, but did not make such a specific assignment. Esters of branched fatty acids are known to require harsher saponification conditions for depolymerization as compared to esters of straight chain fatty acids (Fujii et al., 1986). It is expected that this difficulty would be exacerbated in esters of α -branched fatty acids, due to steric effects. It is possible that under the depolymerization conditions used in previous studies, most of the branched fatty acids remain as components of oligomers and are therefore undetected by gas chromatography.

HSQC correlates the proton chemical shift with that of the carbon to which it is directly attached. The cross-peaks that have been identified in the spectrum (Fig. 2) have been labeled by letters whose assignments are found in Table 1. Cross-peaks B_1 result from CH_2s directly attached to singly bonded ester O atoms and B_2 from CH_2s β to the ester O

atoms. The γ carbon atoms and protons (B_3) are assigned by deduction as part of a large cross-peak that includes other species. The cross-peak labeled C_1 is consistent with CH_2 s α to $C=O$ of esters, and also the same units in fatty acids (F_1). However, the units β to the $C=O$ group in fatty acids or esters (C_2 , F_2) display two signals with a proton shift of 1.5 ppm and carbon shifts of 22 and 25 ppm. Differentiation of these two peaks from the small chemical shift differences in the HSQC is difficult using shifts reported in the literature. However, the cross-peak (1.5, 22 ppm) is missing in cutan, which is obtained after the saponification reaction that cleaves esters (see Fig. 7 later). We believe that the signals in the box labeled ' C_2F_2 ' have significant contribution from esters as well as free acids, with the peak at a ^{13}C shift of 22 ppm that is lost upon saponification assigned to esters (C_2).

In addition to esters, terminal alcohols can also be identified. The carbons and protons in a primary alcohol chain are described by D_1 (CH_2 α to OH), D_2 (β - CH_2), and D_3 (γ - CH_2 , this cross-peak falls under a crowded region that contains cross-peaks from other aliphatic moieties). The *Agave* cutin/cutan mixture does not show peaks for secondary alcohol groups, since a peak attributable to the corresponding methine (3.2, 72 ppm) is absent. Peak G (2.4, 45) is an intense cross-peak consistent with methines in α -branched carboxylic acids or esters. Dostolova et al. (1983) have reported ^{13}C chemical shifts of α -substituted long chain carboxylic acids and esters, which correlate well with the values observed for G. The units β and γ to the functionality in such structures are difficult to distinguish as they coincide with similar units in straight chain esters (C) and fatty acids (F). The main chain methylene and terminal methyl groups in the long polymethylenic chains that contain these ester and acid units are described by cross-peaks A_2 and A_1 , respectively.

In the one-dimensional 1H HRMAS spectrum of cutin/cutan (Fig. 3), the small shoulder around 1 ppm is from terminal methyl groups (A_1), while the largest peak in the spectrum at 1.3 ppm is from main-chain CH_2 (A_2). The ^{13}C NMR spectra (Fig. 4) show an aliphatic region characterized by a small peak at 14 ppm from terminal methyl groups (A_1) and a large peak from main-chain CH_2 (A_2). The main-chain CH_2 groups are composed of both amorphous chains (29 ppm) and crystalline chains (32 ppm) (Hu et al., 2000). Although the CPMAS spectrum shows almost equal quantities of the two entities, the Bloch decay spectrum, indicates a higher peak intensity for the amorphous domains. This is mainly because the amorphous domains are under-represented in the CPMAS spectrum due to lower cross-polarization efficiency on account of their mobility. Assignments of other signals in the ^{13}C and 1H spectra can be made on the basis of the two-dimensional data. The carboxyl

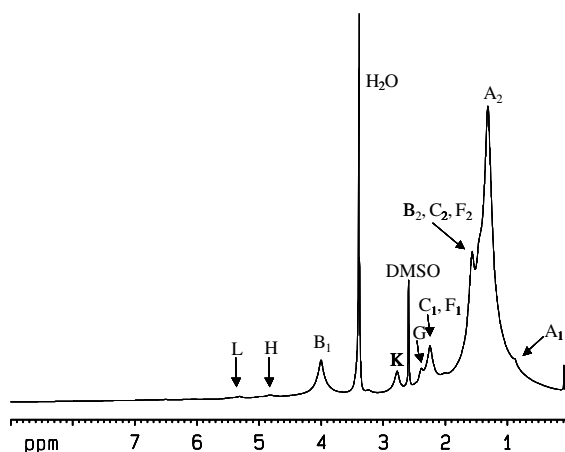


Fig. 3. High resolution magic angle spinning (HRMAS) 1H NMR spectrum of *Agave americana* cutin/cutan mixture, swollen in $DMSO-d_6$, while spinning at 9 kHz.

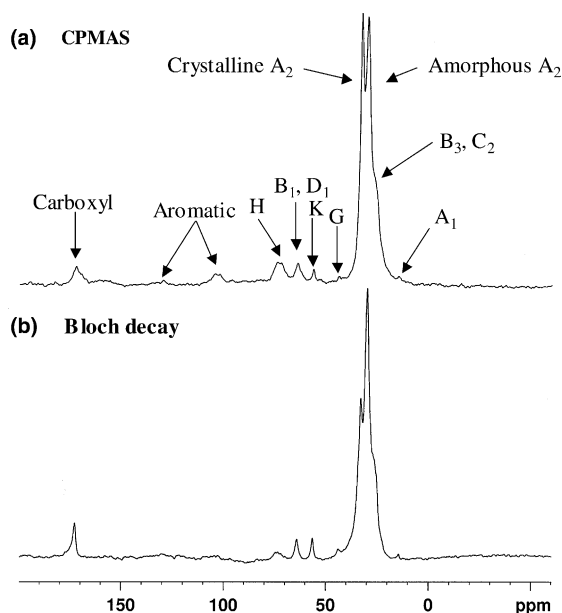
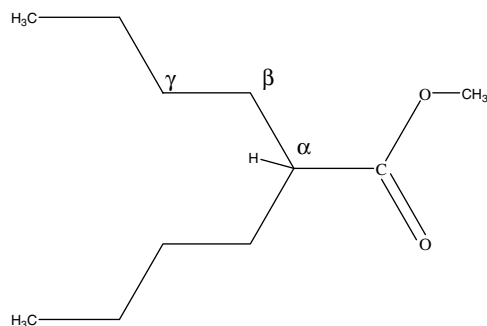


Fig. 4. Solid-state (a) cross-polarization magic angle spinning (CPMAS) ^{13}C NMR spectrum of *Agave americana* cutin/cutan mixture while spinning at 13 kHz, with ramp-CP contact time of 2 ms, recycle delay of 1 s, and spectral width of 27 kHz. (b) Bloch decay ^{13}C NMR spectrum of *Agave americana* cutin/cutan mixture while spinning at 13 kHz, pulse angle of 18° , recycle delay of 2 s, and spectral width of 27 kHz.

(172 ppm) and aromatic (105, 160 ppm) signals seen in the ^{13}C spectra, and the olefinic signals (5.2 ppm) seen in the 1H spectra are the other signals that can be assigned to the indicated structures in Table 1.

The NMR spectra of the *Agave* cutin/cutan mixture are dominated by signals from cutin. This is to be

expected, since the yield of cutan is less than 30% of the starting material. The special feature of *Agave* cutin is the presence of epoxide groups, which is evident in the TOCSY spectrum and which is confirmed by the HSQC data. There is also evidence for α -branched carboxylic acids (G), both in the TOCSY and in the HSQC, which have not been identified before in *Agave* cutin but found to be present only recently in tomato cutin (Deshmukh et al., 2003). Such functionalities are likely sites for cross-linking and are probably responsible for the existence of amorphous chains in the cutin/cutan mixture. A high degree of cross-linking does not allow long chain polymethylenes to line up in a *trans* configuration that leads to high crystallinity.



To further corroborate the ^1H NMR assignment for the α -branched fatty acids, we performed computational studies and employed efficient chemical shift assignment programs to support the experimental assignment at 2.4 ppm. Using a truncated model shown above for the α -branched carboxyl linkage, we computed the optimized geometry of two different conformers of the methyl ester above, and then computed the NMR chemical shifts using density functional theory. The fully optimized

geometries were computed at the B3LYP/6-31G(d) level of theory in the gas phase, and then the ^{13}C and ^1H NMR chemical shifts were computed with the GIAO algorithm (Cheeseman et al., 1996) and the B3LYP/6-311+G(2d,p) level of theory (Becke, 1993; Hehre et al., 1986; Lee et al., 1988; Miehlich et al., 1989) in conjunction with the Gaussian 03 suite of programs (Frisch et al., 2004). For these calculations, tetramethylsilane (TMS) was used as a reference and computed in the analogous fashion.

As shown in Fig. 5, the two conformers differed with respect to the orientation of the methine (C–H) group relative to the C=O group of the ester. The more stable conformer was structure **A**, and it was favored by only 0.6 kcal/mol over structure **B** in the gas phase. Each of the two conformers generate slightly different values for the ^{13}C and ^1H NMR chemical shifts, but in general, they are quite similar for their average values of the chemical shifts (Table 2). In particular, the α -branched methine C–H is calculated to have a ^1H NMR chemical shift of 2.07 to 2.14 ppm in conformers **A** and **B**, respectively. In conformer **B**, the methine C–H is eclipsed to the C=O group and appears further downfield in the spectrum. These calculated chemical shifts are in reasonable agreement with the experimentally observed values for the cuticular materials, especially when one recognizes that the chemical shift of the α methine is highly dependent on the orientation of the carbonyl group and that this orientation could be determined by the cross-linking of the long alkyl chains of the biopolymer.

We also employed an efficient software program from Spectrum Research, LLC (Madison, WI, USA) to predict the chemical shifts for the α methine group as well as the β and γ methylenes of a structure similar to that shown above but having a nine-carbon alkyl

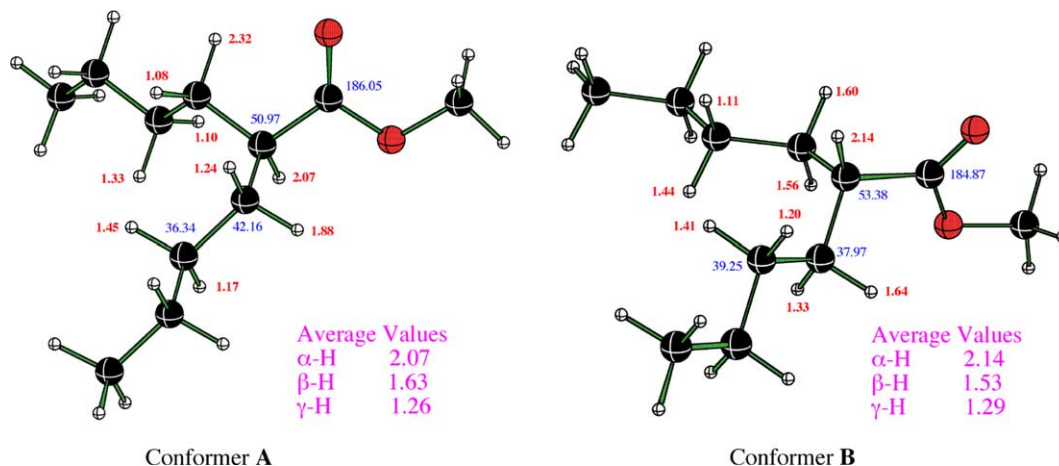


Fig. 5. Calculated structures and chemical shifts (B3LYP/6-311+G(2d,p)//B3LYP/6-31G(d), relative to tetramethylsilane) for the two conformers (**A** and **B**) of the cutin model.

Table 2

Average values of the ^{13}C and ^1H NMR chemical shifts (ppm) for cutin model conformers **A** and **B** relative to tetramethylsilane at the B3LYP/6-311+G(2d,p)//B3LYP/6-31G(d) level of theory^a

Position	Conformer A		Conformer B	
	^{13}C	^1H	^{13}C	^1H
C=O	186.05	–	184.87	–
α -C	50.97	–	53.38	–
β -C	42.16	–	37.97	–
γ -C	36.34	–	39.25	–
α -H (C–H)	–	2.07	–	2.14
β -H (CH ₂)	–	1.63	–	1.53
γ -H (CH ₂)	–	1.26	–	1.29

Density functional theory: Parr and Yang (1989).

B3LYP/6-31G* method: Becke (1993); Miehlich et al. (1989), Lee et al. (1988), Hehre et al. (1986).

GIAO algorithm: Cheeseman et al. (1996).

Gaussian 03: Frisch et al. (2004).

^a See Fig. 5 for the structures of **A** and **B**.

ester group rather than the methyl ester. Both carbon and proton chemical shifts match well with those listed for structure **G** in Table 1. The assignments for cross-correlated protons in the TOCSY spectrum also match well with predicted values of 1.5 and 1.2 ppm for the β and γ protons, respectively.

Some of the assignments can be confirmed using heteronuclear multiple bond correlation (HMBC) NMR spectroscopy, but the HMBC is at least two orders of magnitude less sensitive than HSQC. The ^1H signals are weak even in the HSQC and our efforts to obtain an HMBC spectrum were not successful. Although glycerol has been identified as a product of depolymerization of cutins, its concentration is very low in tomato cutin (Graca et al., 2002). While unesterified glycerol shows chemical shifts of (3.7, 67 ppm) and (3.4, 78 ppm) for the CH₂ and CH units, when esterified, the same units have chemical shift of (4.3, 62–66 ppm) and (5.2, 68–75 ppm), respectively. There are no visible signals in this region of Fig. 2, and it is likely that they are below the detection limit.

3.2. *Agave cutan*

Cutan is the non-extractable and non-hydrolyzable component of the *A. americana* cuticle. The TOCSY spectrum of *A. americana* cutan (Fig. 6) shows evidence for methylenes directly attached to the carboxyl groups in aliphatic fatty acids/esters (F-type) from the peak at 2.2 ppm, which is coupled to protons at 1.5 ppm (β CH₂) and 1.2 ppm (γ CH₂). In order to differentiate between esterified and unesterified acids it is necessary to examine signals from the β CH₂ units in the HSQC spectrum (carbon shift of 22 and 25 ppm, respectively, C₂, F₂

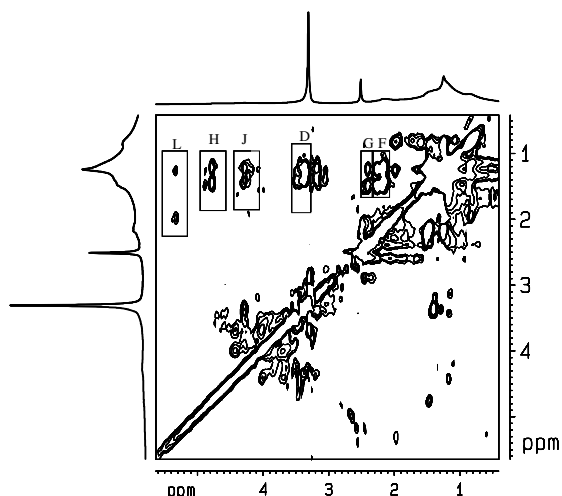


Fig. 6. High resolution magic angle spinning (HRMAS) ^1H – ^1H total correlation spectroscopy (TOCSY) NMR spectrum of *Agave americana* cutan, swollen in DMSO-*d*₆, while spinning at 9 kHz.

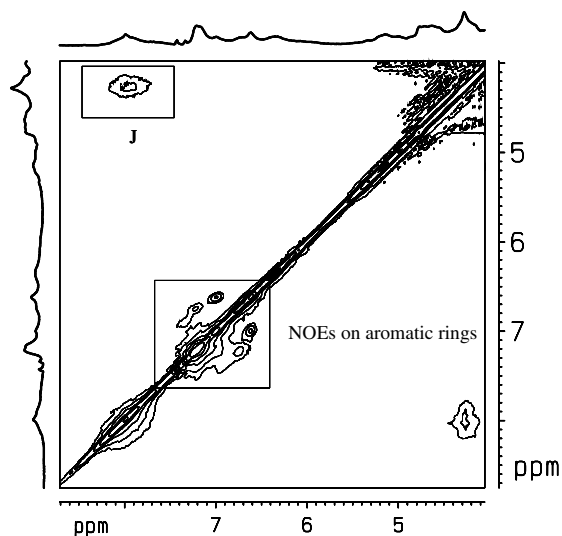


Fig. 7. High resolution magic angle spinning (HRMAS) ^1H – ^1H nuclear Overhauser effect spectroscopy (NOESY) NMR spectrum of *Agave americana* cutan, swollen in DMSO-*d*₆, while spinning at 9 kHz.

in Fig. 2). The peak at 22 ppm in the HSQC spectrum of the cutin/cutan mixture is lost during saponification, and is absent in the HSQC spectrum of cutan (see below). This suggests that, the resonance at 22 ppm results from an ester linkage. The peak at 25 ppm is not affected by saponification, indicative of either the presence of unesterified acids or a different kind of ester. This appears to suggest that cutan may not contain esters

and this contrasts with the structural model of cutan proposed by McKinney et al. (1996) which contains C₇–C₃₁ *n*-alkyl carboxylic acid groups that form esters with phenolic hydroxyls in 1,3,5-trihydroxylated aromatic structures. However, in esters derived from the coupling of phenols and aliphatic fatty acids, the cross-peak for the CH₂ unit β to the ester CO (C₂) is shifted from 22 ppm to 25 ppm due to the presence of the electron-withdrawing aromatic ring. This resonance overlaps that of the cross-peak F₂ normally assigned to the β CH₂ of unesterified long-chain fatty acids. Thus, we conclude that the cross-peak at (1.5, 25) is indeed that of a phenolic ester of the type described by McKinney et al. (1996), with some undetermined contribution from β CH₂s of long-chain fatty acids.

The peak at 2.4 ppm (labeled G in Fig. 6) is from α-branched carboxylic acids, which couples to protons at 1.5 and 1.2 ppm (α and β CH₂ units, respectively). The cross-peak labeled D at 3.3 ppm is from CH₂ units α to the free terminal hydroxyls in long-chain primary alcohols (D₁ in Table 1), which are released from ester linkages during the saponification reaction. ω-Hydroxy fatty acids are known to be released as monomers in the saponification of cutin. Their presence in cutan has not been described. Such units could explain the production of dicarboxylic acids from RuO₄ oxidation of cutan (Schouten et al., 1998). The peak at 3.3 ppm couples with peaks at 1.4 and 1.3 ppm (α and β CH₂ units, respectively).

The cross-peak at 4.2 ppm (J) is from methylenes attached to the O of ester-linked aliphatic alcohols (Table 1). It is likely that these alcohols form esters with aromatic carboxylic acids since this peak is somewhat shifted downfield as compared to the corresponding peak in esters formed between long-chain fatty acids and alcohols (B-type, 4.0 ppm). These methylene protons are coupled to protons at 1.4 ppm (β to O), and 1.2 ppm (γ to O). McKinney et al. (1996) obtained benzene carboxylic acid methyl ester derivatives from TMAH thermochemolysis analysis of *Agave* cutan, which could have been released by the transesterification of such esters. There is further evidence for esters of aromatic acids from a NOESY spectrum of cutan (Fig. 7) in the form of through-space NOEs between the aromatic ring protons (8.0 ppm, α to carbon containing CO₂H group) and the protons on the CH₂ groups directly attached to the singly bonded ester O-atom (4.2 ppm). As explained by McKinney et al. (1996) and Schouten et al. (1998), these esters could have survived saponification due to protection afforded by the hydrophobic long-chain *n*-alkyl groups.

The TOCSY cross-peak at 5.2 ppm (Fig. 6) is from protons on olefinic carbons (L-type) that are coupled to protons at 2.0 and 1.3 ppm (α and β CH₂ units, respectively). Finally, the cross-peak at 4.8 ppm is from methine protons that are directly attached to mid-chain

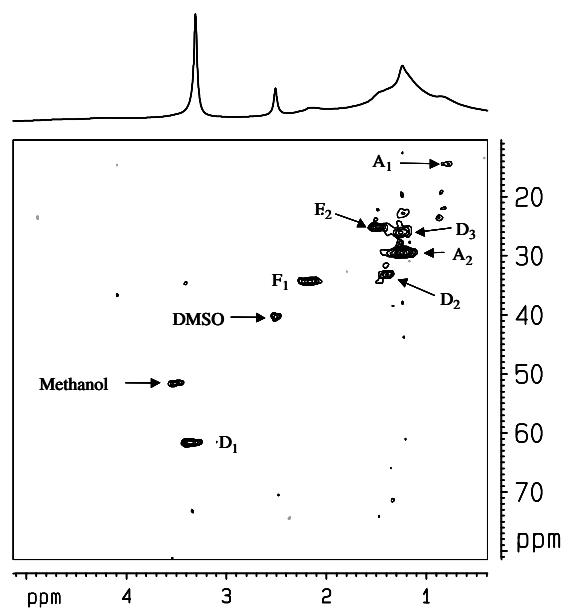


Fig. 8. High resolution magic angle spinning (HRMAS) ¹H–¹³C heteronuclear single quantum coherence (HSQC) NMR spectrum of *Agave americana* cutan, swollen in DMSO-*d*₆, while spinning at 9 kHz.

hydroxyl esters (H-type). This assignment is based on chemical shifts in known compounds (SDBSWeb). This proton is coupled to protons at 1.5 ppm (α protons) and 1.3 ppm (β protons).

The HSQC spectrum of cutan (Fig. 8) shows the presence of several types of C–H systems. The main C–H system is that of methylenes in long-chain alkyl structures. While the small methyl cross-peak indicates that some of these are from long alkyl chains, primary alcohols, as is evident from cross-peaks for CH₂ groups in structures D₁, D₂, and D₃, appear to be significant components, consistent with the TOCSY data. There are also peaks for long-chain carboxylic acids/esters, as seen from cross-peaks F₁ and F₂. These most likely represent long-chain fatty acids that are ester linked to aryl-O systems of the nature described previously (McKinney et al., 1996). Signals for α-branched carboxylic acids, seen in the TOCSY are not observable. Also, other signals seen in the TOCSY spectrum such as esters of aromatic carboxylic acids (J), and esters of mid-chain hydroxyls (H) are not seen. These species are perhaps present at low concentrations and thus are not observable by the HSQC experiment, which is much less sensitive than the TOCSY experiment.

The ¹H spectrum (Fig. 9a) shows a distinct peak for terminal methyl groups at around 0.9 ppm (A₁), and a large peak from main-chain CH₂ characterizes the region between 1.3 and 1.5 ppm. The spectrum shown in Fig. 9(b) was collected using a CPMG sequence with a

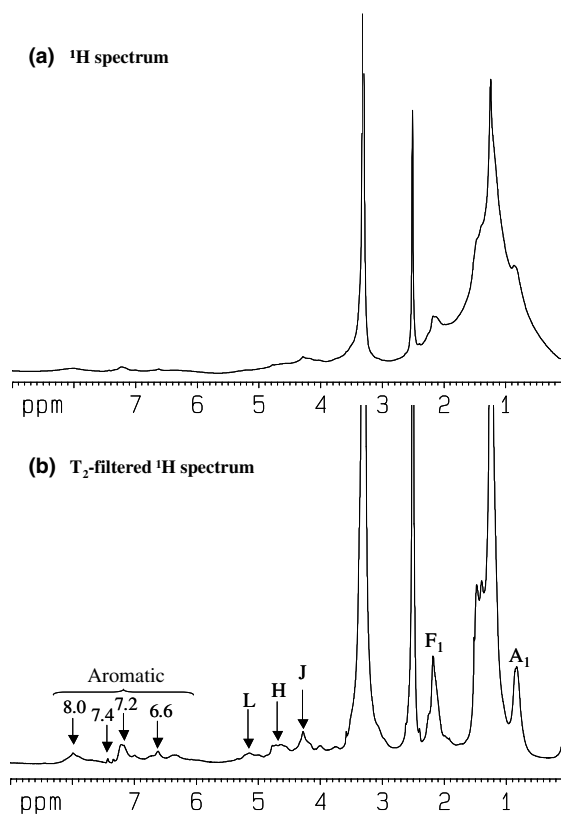


Fig. 9. High resolution magic angle spinning (HRMAS) NMR spectrum of *Agave americana* cutan, swollen in DMSO- d_6 , while spinning at 9 kHz: (a) ^1H -spectrum and (b) T_2 -filtered ^1H -spectrum.

60 μs delay. This acts as a T_2 filter, which helps to remove baseline roll and reduce the linewidth of the peaks. An intense peak from long-chain *n*-alkyl fatty acids (2.2 ppm) is observed, which finds confirmation in the HSQC and TOCSY data. Other proton signals are: aromatic esters (J, 4.2 ppm), esters of mid-chain hydroxyls (H, 4.8 ppm), and olefinic protons (L, 5.2 ppm). Signals from aromatic protons are observed at 6.6, 7.2, 7.4, and 8.0 ppm.

The ^{13}C spectra of cutan (Figs. 10a,b) show a small peak at 14 ppm from terminal methyl groups (A_1) and a large signal for the main-chain CH_2 (A_2). This signal is made up of a dominant peak at 32 ppm for the crystalline polymethylene chains, and a shoulder at 29 ppm for the amorphous chains. Both the CPMAS and Bloch decay spectra are virtually identical, except for the signal-to-noise ratio, and show that the crystalline polymorph is the dominant structural motif for alkyl groups in cutan. Some of the other aliphatic peaks (D_1 and H) have been assigned on the basis of the two-dimensional data (Table 1). The remaining peaks include aromatic signals at 105 ppm (H–Ar), 107 ppm

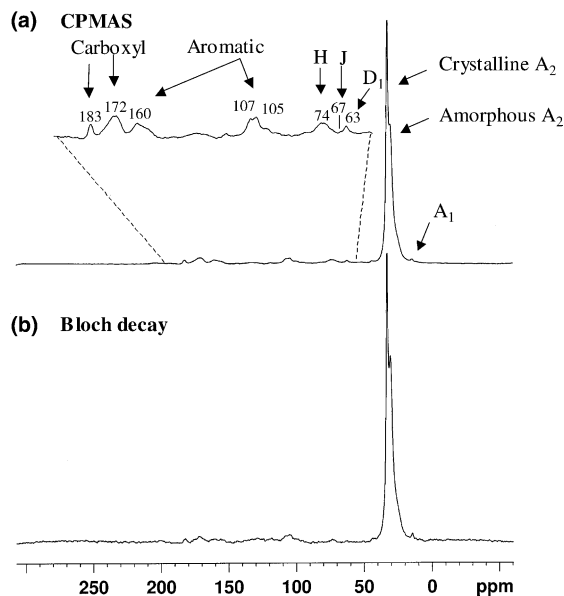


Fig. 10. Solid-state (a) cross-polarization magic angle spinning (CPMAS) ^{13}C NMR spectrum of *Agave americana* cutan while spinning at 13 kHz, with ramp-CP contact time of 2 ms, recycle delay of 1 s, and spectral width of 27 kHz. (b) Bloch decay ^{13}C NMR spectrum of *Agave americana* cutan while spinning at 13 kHz, pulse angle of 18° , recycle delay of 2 s, and spectral width of 27 kHz.

(H–Ar), 160 ppm (O–Ar), and carboxyl at 172 ppm, as assigned before (McKinney et al., 1996). In addition, the peak at 183 ppm is probably derived from carboxylic functionalities as well. McKinney et al. (1996) had originally assigned this peak as ketone, but there is no evidence for ketones from the present two-dimensional data.

There may be different types of hydroxylated aromatic ring systems in the *Agave* cutan backbone. McKinney et al. (1996) showed the presence of trihydroxylated (*meta* to each other) benzene rings that form ester linkages with fatty acids from NMR and TMAH analysis. We have been able to suggest the existence of benzene carboxylic acids in ester linkages with fatty alcohols. 3,5-Dimethoxy benzoic acid methyl ester was a significant product obtained in the TMAH analysis by McKinney et al. (1996), and the peaks seen in the aromatic region of the one-dimensional ^1H spectrum support such a structure. Figure 11 shows possible structures for monomer units in cutan with the predicted ^1H chemical shifts.

4. Conclusions

What differentiates *Agave* cutin from other well-studied cutins, such as tomato and lime fruit cuticles, is the presence of epoxide groups. The predominant

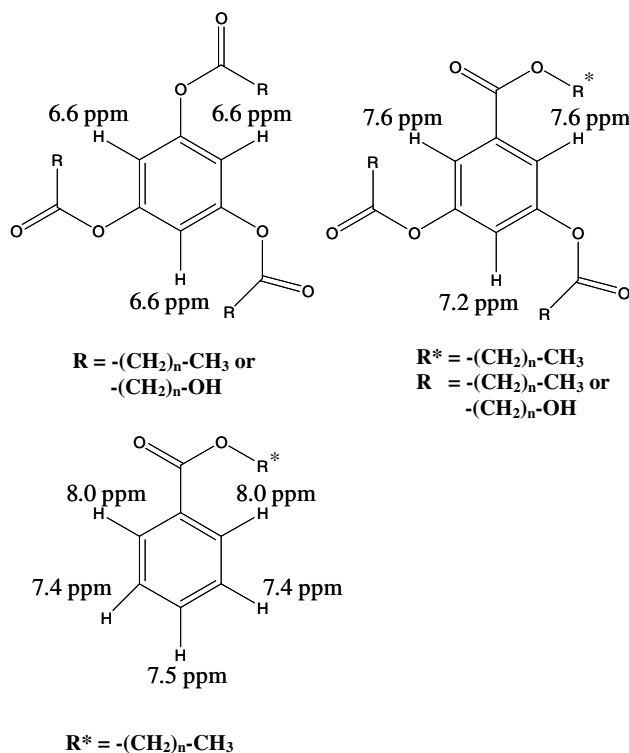


Fig. 11. Proposed monomer structural units in *Agave americana* cutan, with chemical shifts for aromatic protons shown.

signals are from ester linkages, although the spectra also show the presence of free terminal alcohols and olefinic carbons. The α -branched carboxylic acids, which have been identified in cuticles only in the recent past (Deshmukh et al., 2003), were also found in these cuticles. Such functionalities offer opportunities for cross-linking, and are the explanation for the presence of amorphous chains in the cutin/cutan mixture.

Blee (1998) has suggested a mechanism for cross-linking in cutin, resulting in more condensed regions, i.e., cutan, through reactions between epoxy groups and hydroxy substituents of adjacent cutin monomers, leading to ether bonds. However, a cross-peak at (3.5, 70 ppm) in the HSQC spectrum expected from methylenes adjacent to the O atoms in such ether bonds, is not observed. After evaluating the current dataset as well as the data available in the literature, we do not believe that ether linkages exist in cutan as believed by Blee (1998) and Villena et al. (1999). We have been able to uncover an important structural unit in the non-saponifiable and non-extractable biopolymer cutan found in the *A. americana* leaf cuticles. The revised structure of cutan proposed by us (Fig. 12) has an aromatic backbone as before, but with additional carboxylic acid functionalities, along with the previously

proposed aromatic hydroxy (phenolic) functionalities. These groups form ester linkages with long-chain alcohols, and long-chain carboxylic acids, respectively. The model incorporates units that include α -branched carboxylic acids (G), esterified secondary alcohols (H), free primary alcohols (D), and olefinic linkages. We have retained the C_7 linker in our model, which was previously proposed by Schouten et al. (1998), and which explains the predominant C_9 dicarboxylic acid product during RuO_4 treatment.

Acknowledgments

This research was supported with research funding from the National Science Foundation (NSF) to the Environmental Molecular Science Institute (EMSI) at the Ohio State University (Grant # CHE-0089147). We also thank Anne McCullough at the Franklin Park Conservatory, Columbus, OH, for providing *Agave americana* leaves. The manuscript benefited greatly from editorial comments by Heike Knicker (Technical University, Munich) and Pierre Metzger (CNRS, Paris).

Associate Editor—G. Abbott

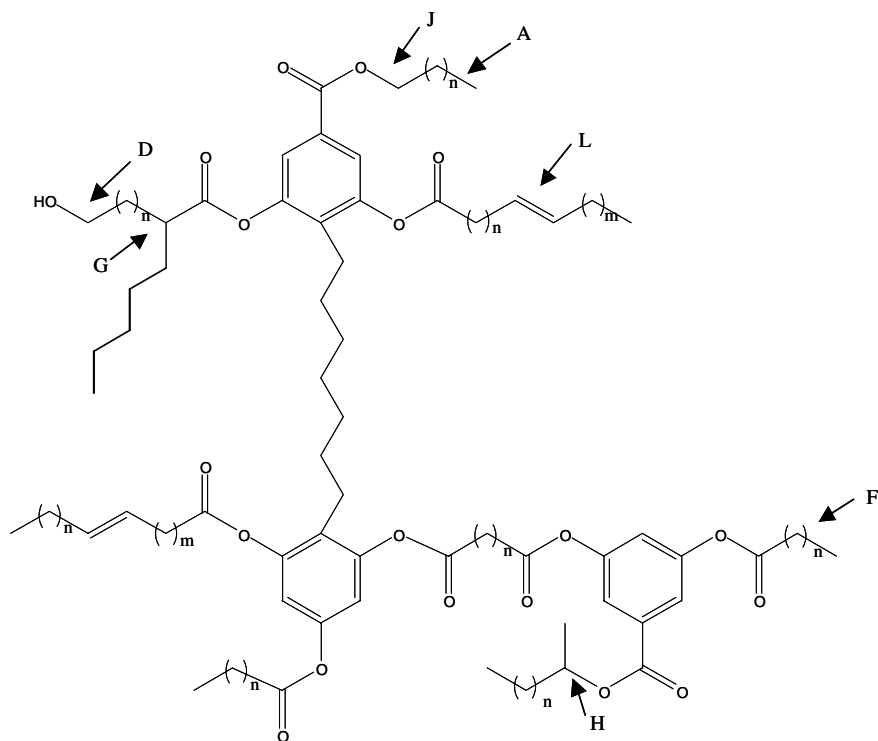


Fig. 12. Proposed structure for *Agave americana* cutan, shown with the various types of functional units (A–L) that are listed in Table 1. The units for n vary from 25 to 32 based on the work of Schouten et al. (1998) and McKinney et al. (1996). Values for m are at least 6 to allow sufficient remoteness from the carbonyl group to display a chemical shift assignable to L structures. Values of $m + n$ are less than 31.

References

- Baldock, J.A., Oades, J.M., Nelson, P.N., Skene, T.M., Golchin, A., Clark, P., 1997. Assessing the extent of decomposition of natural organic materials using solid-state ^{13}C NMR spectroscopy. *Australian Journal of Soil Research* 35, 1061–1083.
- Becke, A.D., 1993. A new mixing of Hartree–Fock and local-density-functional theories. *Journal of Chemical Physics* 98, 1372–1377.
- Bennett, A.E., Rienstra, C.M., Auger, M., Lakshmi, K.V., Griffin, R.G., 1995. Heteronuclear decoupling in rotating solids. *Journal of Chemical Physics* 103, 6951–6958.
- Blee, E., 1998. Biosynthesis of phytooxylipins: the peroxygenase pathway. *Fett/Lipid* 100, 121–127.
- Blee, E., 2002. Cutin monomers: biosynthesis and plant defense. In: Min, K.T., Gardner, H.W. (Eds.), *Lipid Biotechnology*. Marcel Dekker, New York, NY, pp. 231–248.
- Cheeseman, J.R., Trucks, G.W., Keith, T.A., Frisch, M.J., 1996. A comparison of models for calculating nuclear magnetic resonance shielding tensors. *Journal of Chemical Physics* 104, 5497–5509.
- Collinson, M.E., van Bergen, P.F., Scott, A., de Leeuw, J.W., 1994. The oil-generating potential of plants from coal and coal-bearing strata through time: a review with new evidence from carboniferous plants. In: Scott, A.C., Fleet, A.J. (Eds.), *Coal and Coal-bearing Strata as Oil-prone Source Rocks*. Geological Society, pp. 31–67 (Special Publication No. 77).
- Derenne, S., Lageau, C., 2001. A review of some important families of refractory macromolecules: composition, origin, and fate in soils and sediments. *Soil Science* 166, 833–847.
- Deshmukh, A.P., Simpson, A., Hatcher, P.G., 2003. Evidence for cross-linking in tomato cutin using HR-MAS NMR spectroscopy. *Phytochemistry* 64, 1163–1170.
- Dostolova, V.I., Terenter, A.B., Ikonnikov, N.S., Freidlina, R., Kh, 1983. Carbon-13 NMR spectra and the method for their calculation for long-chain polybranched carboxylic acids and their derivatives. *Organic Magnetic Resonance* 21, 11–19.
- Espelie, K.E., Wattendorf, J., Kolattukudy, P.E., 1982. Composition and ultrastructure of the suberized cell wall of isolated crystal idioblasts from *Agave americana* L. leaves. *Planta* 155, 166–175.
- Fang, X., Qiu, F., Wang, H., Mort, A.J., Stark, R.E., 2001. NMR studies of molecular structure in fruit cuticle polyesters. *Phytochemistry* 57, 1035–1042.
- Fujii, M., Hida, M., Ono, H., Tabata, A., Matsumoto, M., 1986. Improvement of measuring method of saponification

- value on bees wax, etc. Nippon Koshohin Kagakkaishi 10, 269–274.
- Frisch, M.J., Trucks, G.W., Schlegel, H.B., Scuseria, G.E., Robb, M.A., Cheeseman, J.R., Montgomery Jr., J.A., Vreven, T., Kudin, K.N., Burant, J.C., Millam, J.M., Iyengar, S.S., Tomasi, J., Barone, V., Mennucci, B., Cossi, M., Scalmani, G., Rega, N., Petersson, G.A., Nakatsuji, H., Hada, M., Ehara, M., Toyota, K., Fukuda, R., Hasegawa, J., Ishida, M., Nakajima, T., Honda, Y., Kitao, O., Nakai, H., Klene, M., Li, X., Knox, J.E., Hratchian, H.P., Cross, J.B., Bakken, V., Adamo, C., Jaramillo, J., Gomperts, R., Stratmann, R.E., Yazyev, O., Austin, A.J., Cammi, R., Pomelli, C., Ochterski, J.W., Ayala, P.Y., Morokuma, K., Voth, G.A., Salvador, P., Dannenberg, J.J., Zakrzewski, V.G., Dapprich, S., Daniels, A.D., Strain, M.C., Farkas, O., Malick, D.K., Rabuck, A.D., Raghavachari, K., Foresman, J.B., Ortiz, J.V., Cui, Q., Baboul, A.G., Clifford, S., Cioslowski, J., Stefanov, B.B., Liu, G., Liashenko, A., Piskorz, P., Komaromi, I., Martin, R.L., Fox, D.J., Keith, T., Al-Laham, M.A., Peng, C.Y., Nanayakkara, A., Challacombe, M., Gill, P.M.W., Johnson, B., Chen, W., Wong, M.W., Gonzalez, C., Pople, J.A., 2004. Gaussian 03, Revision C.02. Gaussian Inc., Wallingford, CT.
- Graca, J., Schreiber, L., Rodrigues, J., Pereira, H., 2002. Glycerol and glyceryl esters of ω -hydroxyacids in cutins. *Phytochemistry* 61, 205–215.
- Hediger, S., Meier, B.H., Ernst, R.R., 1993. Cross polarization under fast magic angle sample spinning using amplitude modulated spin-lock sequences. *Chemical Physics Letters* 213, 627–635.
- Hehre, W.J., Radom, L., Schleyer, P.v.R., Pople, J.A., 1986. *Ab Initio Molecular Orbital Theory*. Wiley, New York.
- Holloway, P.J., 1984. Cutins and suberins, the polymeric plant lipids. In: Mangold, H.K., Zweig, G., Sherma, J. (Eds.), *CRC Handbook of Chromatography: Lipids*, vol. I. CRC Press, Boca Raton, FL, pp. 321–345.
- Holloway, P.J., 1994. Plant cuticles: physicochemical characteristics and biosynthesis. *NATO ASI Series, Series G: Ecological Sciences (1994)*, 36 (Air Pollutants and the Leaf Cuticle), pp. 1–13.
- Hu, W.-G., Mao, J., Xing, B., Schmidt-Rohr, K., 2000. Poly(methylene) crystallites in humic substances detected by nuclear magnetic resonance. *Environmental Science and Technology* 34, 530–534.
- Jeffrey, C.E., 1996. Structure and ontogeny of plant cuticles. In: Kerstiens, G. (Ed.), *Plant Cuticles an Integrated Functional Approach*. Bios Scientific Publishers Ltd., Oxford, UK, pp. 33–82.
- Keifer, P.A., Baltusis, L., Rice, D.M., Tymiak, A.A., Shoolery, J.N., 1996. A comparison of NMR spectra obtained for solid phase synthesis resins using conventional high-resolution, magic angle spinning probes. *Journal of Magnetic Resonance* 119A, 65–75.
- Kögel-Knabner, I., Ziegler, F., Riederer, M., Zech, W., 1989. Distribution and decomposition pattern of cutin and suberin in forest soils. *Zeitschrift für Pflanzenernährung und Bodenkunde* 152, 409–413.
- Kolattukudy, P.E., 1980. Biopolyester membranes of plants: cutin and suberin. *Science* 208, 990–1000.
- Kolattukudy, P.E., 1984. Biochemistry and function of cutin and suberin. *Canadian Journal of Botany* 62, 2918–2933.
- Kolattukudy, P.E., 2001. Polyesters in higher plants. *Advances in Biochemical Engineering/Biotechnology* 71 (Biopolyesters), 1–49.
- Kolattukudy, P.E., 2002. Cutin from plants. In: Doi, Y., Steinbuechel, A. (Eds.), *Biopolymers*. Wiley-VCH Verlag GmbH, Weinheim, Germany, pp. 1–40.
- Lee, C., Yang, W., Parr, R.G., 1988. Development of the Colle–Salvetti correlation-energy formula into a functional of the electron density. *Physical Reviews B* 37, 785–789.
- McKinney, D.E., Bortiatynski, J.M., Carson, D.M., Clifford, D.J., de Leeuw, J.W., Hatcher, P.G., 1996. Tetramethylammonium hydroxide (TMAH) thermochemolysis of the aliphatic biopolymer cutan: insights into the chemical structure. *Organic Geochemistry* 24, 641–650.
- Miehlich, B., Savin, A., Stoll, H., Preuss, H., 1989. Results obtained with the correlation energy density functionals of Becke and Lee, Yang and Parr. *Chemical Physics Letters* 157, 200–206.
- Millis, K., Maas, W.E., Singer, S., Cory, D.G., 1997. Gradient, high-resolution magic angle spinning nuclear magnetic resonance spectroscopy of human adipocyte tissue. *Magnetic Resonance in Medicine* 38, 399–403.
- Nierop, K.G.J., 1998. Origin of aliphatic compounds in a forest soil. *Organic Geochemistry* 29, 1009–1016.
- Nip, M., Tegelaar, E.W., de Leeuw, J.W., Schenk, P.A., Holloway, P.J., 1986a. A new non-saponifiable highly aliphatic and resistant biopolymer in plant cuticles. Evidence from pyrolysis and ^{13}C NMR analysis of present-day and fossil plants. *Naturwissenschaften* 73, 579–585.
- Nip, M., Tegelaar, E.W., Brinkhuis, H., de Leeuw, J.W., Schenk, P.A., Holloway, P.J., 1986b. Analysis of modern and fossil plant cuticles by Curie-point Py-GC and Curie-point Py-GC-MS: recognition of a new, highly aliphatic and resistant biopolymer. *Organic Geochemistry* 10, 769–778.
- Parr, R.G., Yang, W., 1989. *Density Functional Theory in Atoms and Molecules*. Oxford University Press, New York.
- Riederer, M., Schonherr, J., 1988. Development of plant cuticles: fine structure and cutin composition of *Clivia miniata* Reg. leaves. *Planta* 174, 127–138.
- SDBSWeb: <http://www.aist.go.jp/RIODB/SDBS/> (04/11/03).
- Schouten, S., Moerkerken, P., Gelin, F., Baas, M., de Leeuw, J.W., Sinnighe Damste, J.S., 1998. Structural characterization of aliphatic, non-hydrolyzable biopolymers in freshwater algae and a leaf cuticle using ruthenium tetroxide degradation. *Phytochemistry* 49, 987–993.
- Stark, R.E., Yan, B., Ray, A.K., Chen, Z., Fang, X., Garbow, J.R., 2000. NMR studies of structure and dynamics in fruit cuticle polyesters. *Solid State NMR* 16, 37–45.
- Tegelaar, E.W., de Leeuw, J.W., Largeau, C., Derenne, S., Schulten, H.-R., Muller, R., Boon, J.J., Nip, M., Sprengels, J.C.M., 1989. Scope and limitations of several pyrolysis methods in the structural elucidation of a macromolecular plant constituent in the leaf cuticle of *Agave americana* L. *Journal of Analytical Applied Pyrolysis* 15, 29–54.
- Tegelaar, E.W., Hollman, G., van der Vegt, P., de Leeuw, J.W., Holloway, P.J., 1995. Chemical characterization of periderm tissue of some angiosperm species: recognition of an insoluble, non-hydrolyzable, aliphatic biomacromolecule (suberan). *Organic Geochemistry* 23, 239–250.

- Tegelaar, E.W., Kerp, H., Visscher, H., Schenck, P.A., de Leeuw, J.W., 1991. Bias of the paleobotanical record as a consequence of variations in the chemical composition of higher vascular plant cuticles. *Paleobiology* 17, 133–144.
- van Bergen, P.F., Scott, A.C., Barrie, P.J., de Leeuw, J.W., Collinson, M.E., 1994. The chemical composition of upper carboniferous pteridosperm cuticles. *Organic Geochemistry* 21, 107–112.
- Villena, J.F., Dominguez, E., Stewart, D., Heredia, A., 1999. Characterization and biosynthesis of non-degradable polymers in plant cuticles. *Planta* 208, 181–187.
- Zeliber, J.L.J., Romankiw, L., Hatcher, P.G., Colwell, R.R., 1988. Comparative analysis of the chemical composition of mixed and pure cultures of green cultures algae and their decomposed residues by carbon-13 nuclear magnetic resonance spectroscopy. *Applied and Environmental Microbiology* 54, 1051–1060.